# Supporting Information

## Non-Equilibrium Preparation of (*E*)-Phosphinimine (HPNH, $X^1A'$) – A Precursor to Prebiotic Phosphorylating Agents

Jia Wang,[1,2] Bing-Jian Sun,[3] Alexandre Bergantini,[1,2,5] Zesen Wang,[1,2] Mason McAnally,[1,2] Joshua H. Marks,[1,2] Agnes H. H. Chang,[3*] André K. Eckhardt,[4*] Ralf I. Kaiser[1,2*]

[1] W. M. Keck Research Laboratory in Astrochemistry, University of Hawaii at Manoa, Honolulu, Hawaii 96822, United States

[2] Department of Chemistry, University of Hawaii at Manoa, Honolulu, Hawaii 96822, United States

[3] Department of Chemistry, National Dong Hwa University, Shoufeng, Hualien 974, Taiwan

[4] Lehrstuhl für Organische Chemie II, Ruhr-Universität Bochum, Bochum 44801, Germany

[5] Present address: Centro Federal de Educacao Tecnologica Celso Suckow da Fonseca-CEFET-RJ, Av. Maracana 229, 20271-110, Rio de Janeiro, Brazil

[*]Corresponding Authors:

Agnes H. H. Chang, hhchang@gms.ndhu.edu.tw

André K. Eckhardt, Andre.Eckhardt@ruhr-uni-bochum.de

Ralf I. Kaiser, ralfk@hawaii.edu

## Methods

**Experimental**. All experiments were conducted in an ultrahigh vacuum chamber with base pressures of a few $10^{-11}$ Torr, achieved using magnetically suspended turbomolecular pumps backed by an oil-free scroll pump.[1] A polished silver substrate was mounted to a cold head connected to a closed-cycle helium compressor (Sumitomo Heavy Industries, RDK-415E). The cold head can be moved vertically and rotated about the vertical axis.[1] Experimental procedures have been described in detail previously.[2] Phosphine ($PH_3$, Sigma-Aldrich, 99.9995%), ammonia ($NH_3$, Matheson, 99.9992%), and isotopically labeled ammonia-$^{15}N$ ($^{15}NH_3$, Sigma-Aldrich, 98% $^{15}N$) were used. Once the silver substrate reached 5 K, phosphine and ammonia were co-deposited onto the substrate via a pair of glass capillary arrays with partial pressures of $1\times 10^{-8}$ Torr for each reactant. Utilizing laser interferometry with a helium-neon laser (632.8 nm),[3] the thickness of the deposited $PH_3$–$NH_3$ ice was calculated to be 1410 ± 50 nm; the ratio of phosphine to ammonia was estimated to be (1.6 ± 0.5):1 based on the integrated infrared absorption and absorption coefficients of reactants.[2] The absorption coefficients of $5.1 \times 10^{-19}$ cm molecule$^{-1}$ of $PH_3$ ($\nu_2$)[3] and $5.6 \times 10^{-18}$ cm molecule$^{-1}$ for $NH_3$ ($\nu_4$)[4,5] were used. Infrared spectra were collected via a Fourier Transform Infrared (FTIR) spectrometer (Nicolet 6700) with a resolution of 4 cm$^{-1}$. After deposition, the $PH_3$–$NH_3$ ice mixtures were exposed to energetic (5 keV) electrons at a current of 20 nA for 15 minutes. These electrons simulate secondary electrons produced by GCRs as they pass through the interstellar ices in a molecular cloud.[6] The irradiation doses of 0.8 ± 0.2 eV per $PH_3$ molecule and 0.4 ± 0.1 eV per $NH_3$ molecule[2,7] simulate the energy input by GCRs over timescales equivalent to lifetimes of up to $3\times 10^6$ years for cold molecular clouds,[8] corresponding to their early evolutionary stage. Utilizing the densities of $PH_3$ (0.90 g cm$^{-3}$)[3,9] and $NH_3$ (0.74 g cm$^{-3}$),[4] approximately 99% of the incident electron energy was deposited within the upper 700 ± 50 nm of the ice mixture using CASINO 2.42;[7] this penetration depth is much less than the total ice thickness, ensuring that electrons do not interact with the substrate.

After irradiation, the ices were warmed from 5 to 320 K at a ramping rate of 1 K min$^{-1}$ during temperature-programmed desorption (TPD). As molecules sublime, they are photoionized by pulsed VUV photons generated via the four-wave mixing method in a krypton/xenon gas jet (30 Hz).[10] The generation parameters for photon energies of 10.49, 9.47, and 8.80 eV are listed in Table S3. Specifically, 10.49 eV photons were produced by tripling the third harmonic (355 nm) of an Nd:YAG laser (Spectra-Physics, Quanta Ray PRO 250-30) in xenon gas. To generate 9.47

eV photons, the third harmonic of an Nd:YAG laser (Spectra-Physics, Quanta Ray PRO 270-30) pumped a dye laser (Sirah Lasertechnik, Cobra-Stretch) operating with stilbene 420 dye, yielding 212.556 nm ($\omega_1$) after second harmonic generation with a beta-barium borate (BBO) crystal. Meanwhile, a separate Nd:YAG laser pumped a dye laser operating with the Rhodamine 590 dye to generate 564.583 nm ($\omega_2$). The combination of $2\omega_1$ and $\omega_2$ in krypton gas produced 9.47 eV photons via four-wave difference frequency mixing. The 9.39 eV or 8.80 eV photons were generated in xenon gas using $\omega_1$ = 222.566 nm and $\omega_2$ = 707.956 nm or 529.553 nm. The $\omega_1$ beam was obtained by frequency doubling 445.132 nm light from Coumarin 450 dye pumped by the third harmonic (355 nm) of an Nd:YAG laser, while $\omega_2$ was produced by pumping Coumarin 450 dye with the second harmonic (532 nm) of another Nd:YAG laser. The output wavelengths of the dye lasers were calibrated using a wavelength meter (Coherent, WaveMaster) with an accuracy of 0.1 $cm^{-1}$, resulting in an uncertainty of less than 0.001 eV in the photon energy. The VUV photons were separated from the dye laser beams using a biconvex lithium fluoride lens in an off-axis configuration and directed to pass 2.0 ± 0.5 mm above the substrate surface. VUV photons ionize molecules via single-photon ionization, which produces exclusively singly charged cations. The resulting ions were detected using a reflectron time-of-flight mass spectrometer (ReToF-MS, Jordan TOF Products, Inc.). Ion signals were amplified with a preamplifier (Ortec 9305) and collected using a multichannel scaler (FAST ComTec, MCS6A). Each mass spectrum was accumulated over 3600 sweeps (2 minutes) during the temperature-programmed desorption process.

**Computational**. The coupled cluster[11-14] CCSD/cc-pVTZ calculations are carried out to obtain optimized geometries, harmonic vibrational frequencies, and infrared intensities of neutral $H_2PN$ isomers and cations. The energies are refined by computing coupled cluster CCSD(T)/cc-pVDZ, CCSD(T)/cc-pVTZ, and CCSD(T)/cc-pVQZ energies, which are extrapolated to completed basis set limits,[15] CCSD(T)/CBS, with CCSD/cc-pVTZ zero-point energy corrections. The adiabatic ionization energies (IEs) are calculated by taking the difference in energies between the ionic and the neutral states of similar conformation. The Cartesian coordinates, harmonic vibrational frequencies, and infrared intensities of the computed structures are provided in Tables S4–S9. To assess whether the single-reference coupled cluster methods are appropriate for the present system, the $T_1$ diagnostic[16,17] is examined for both close-shell and open-shell species in Figs. 1, 4, and 6. As seen in Table S10, for the close-shell species **4**, **ts (6**–**3**+$H_2$**)**, and the open-shell species (*E*)-$\mathbf{3}^+$,

(*Z*)-**3**$^+$, and **4**$^+$, the $T_1$ diagnostic values are exceed 0.02, and 0.044, respectively, which may indicate appreciable multi-reference character. Thus, the multi-reference configuration interaction (MRCI) calculations are also performed based on the CCSD/cc-pVTZ optimized geometries of (*E*)-**3**, (*E*)-**3**$^+$, (*Z*)-**3**, (*Z*)-**3**$^+$, **4**, **4**$^+$, **6**, and **ts** (**6**–**3**+$H_2$). The reference space and molecular orbitals are provided by MCSCF (6,9)/(5,9), 6 (or 5) active electrons in 9 orbitals for neutrals and cations, respectively. Likewise, MRCI/cc-pVDZ, MRCI/cc-pVTZ, and MRCI/cc-pVQZ energies with Davidson corrections are extrapolated to yield the MRCI/CBS energies with CCSD/cc-pVTZ zero-point energy corrections as shown in Table S11. The Gaussian 16 program is employed in the *ab initio* electronic structure calculations,[18] and MOLPRO[19] is used for the computations of MCSCF, and MRCI. It is important to note that combined error bounds of −0.03/+0.06 eV are applied to the calculated IEs based on the benchmarking against experimental and calculated IEs of molecular systems.[20] The ionization energies are subject to small shifts due to Stark effects in the photoionization region with an extraction electric field of 200 V cm$^{-1}$ and from the internal thermal energy of the desorbing molecules at 153 K; these contributions are estimated to result in a combined shift of approximately −0.03 eV, comprising for the thermal (−0.014 eV) and Stark effects (−0.011 eV).[21] The ultraviolet-visible (UV-Vis) spectra of (*E*)-**3**, (*Z*)-**3**, and **4** were calculated at the TD-B3LYP/cc-pVTZ level of theory.

**Evidence for the formation of hydrazine ($N_2H_4$) and diphosphine ($P_2H_4$)**

At 10.49 eV, the TPD profile of the ion signal at *m/z* = 32 from irradiated $PH_3$–$NH_3$ ice reveals three sublimation events peaking at 79, 115, and 165 K (Fig. S5a). The blank experiment shows a sublimation event at 79 K, indicating that this peak is likely due to contamination in the samples. Given the molecular weights of the reactants, the ion signal of *m/z* = 32 could be attributed to $PH^+$ and/or $N_2H_4^+$. When the $PH_3$–$NH_3$ ice is replaced with $PH_3$–$^{15}NH_3$ ice, the TPD profile of *m/z* = 34 exhibits a broad, saturated sublimation feature between 60 and 140 K due to the $PH_3$ reactant, along with a later peak at 165 K, suggesting that this higher-temperature event can be attributed to an $N_2H_4$ isomer. Previous studies of electron-irradiated ammonia–water ($NH_3$–$H_2O$) ices at 10 and 50 K suggested that hydrazine ($N_2H_4$) sublimes at a peak temperature of 170 K,[22] supporting the assignment of the 165 K peak to hydrazine.

In addition, the TPD profile of *m/z* = 66 from irradiated $PH_3$–$NH_3$ ice at 10.49 eV reveals a strong sublimation event peaking at 122 K (Fig. S5b). No sublimation event is observed at *m/z* = 66 in the blank experiment, indicating that this event originates from electron-induced processing of the ice. Considering the molecular weights of the reactants, the ion signal at *m/z* = 66 can only be assigned to a species with the molecular formula $P_2H_4$. Substitution of $PH_3$–$NH_3$ ice with $PH_3$–$^{15}NH_3$ ice results in no mass shift of the TPD profile, indicating the absence of nitrogen incorporation and further confirming the assignment to $P_2H_4$. Previous studies on electron-irradiated phosphine ices at 5 K reported that diphosphine ($P_2H_4$) sublimes with a strong event peaking at 121 K,[3] which closely matches our result (122 K), supporting the assignment of this sublimation peak to diphosphine.

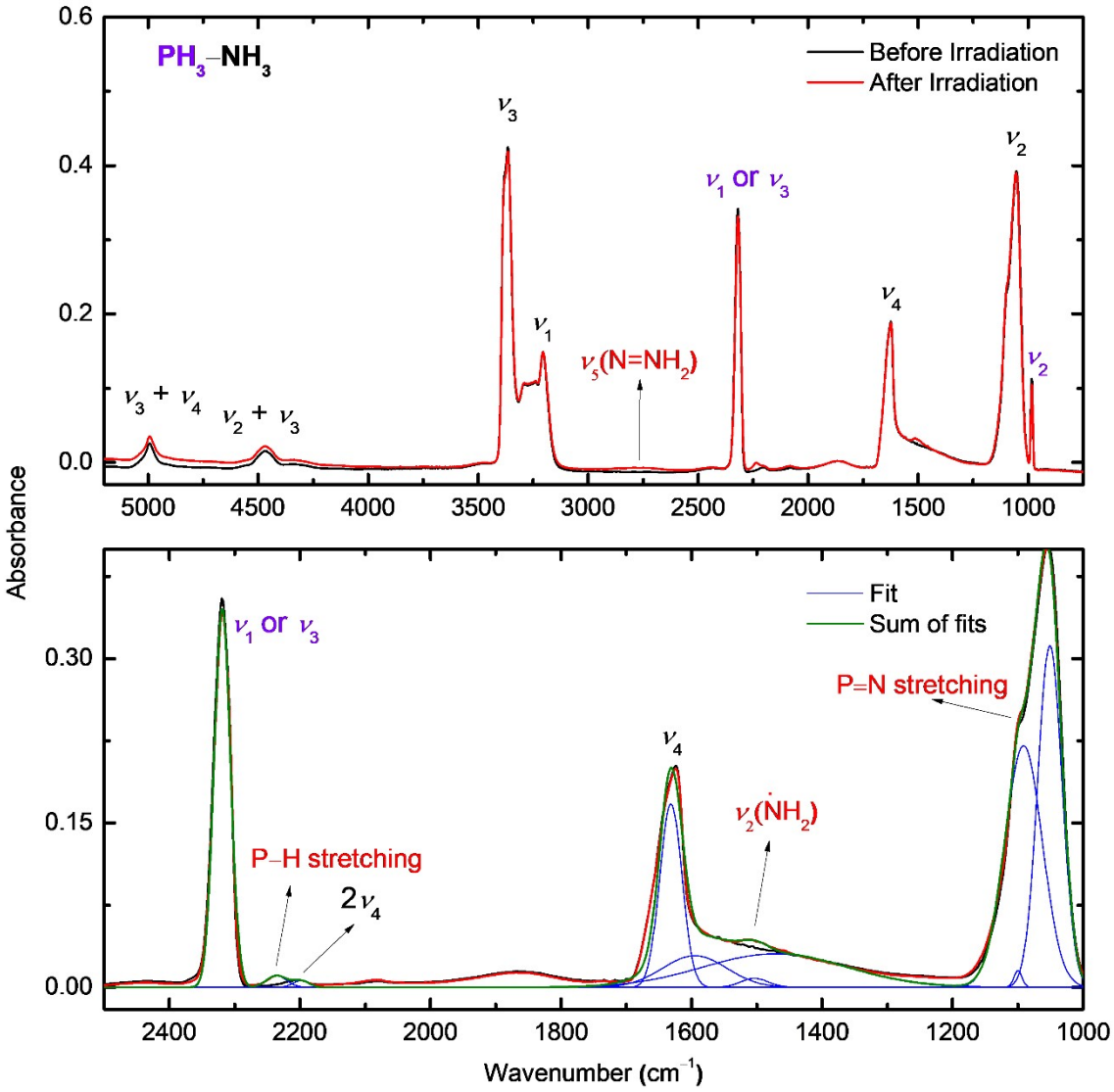


**Figure S1**. Infrared spectra of $PH_3$–$NH_3$ ice before and after electron irradiation at 5 K. The bottom panel shows a magnified, baseline-corrected view of the 2500–1000 $cm^{-1}$ region with Gaussian deconvolution. Assignments of absorptions of $PH_3$, $NH_3$, and new features are indicated in purple, black, and red, respectively. Detailed band assignments are provided in Table S1.

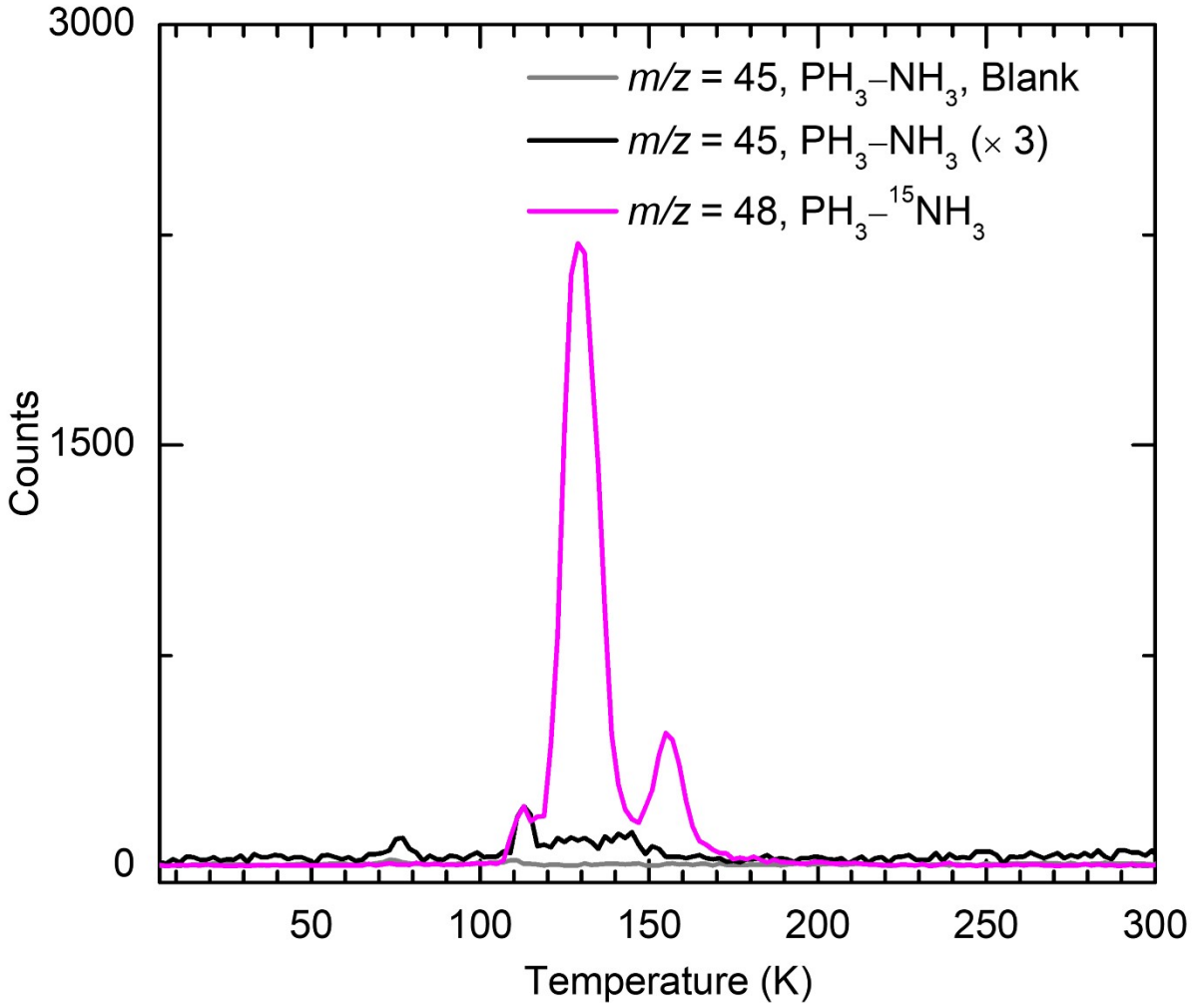


**Figure S2**. TPD profiles of *m/z* = 45 from blank and irradiated $PH_3$–$NH_3$ ices, and *m/z* = 48 from irradiated $PH_3$–$^{15}NH_3$ ices measured at 10.49 eV.

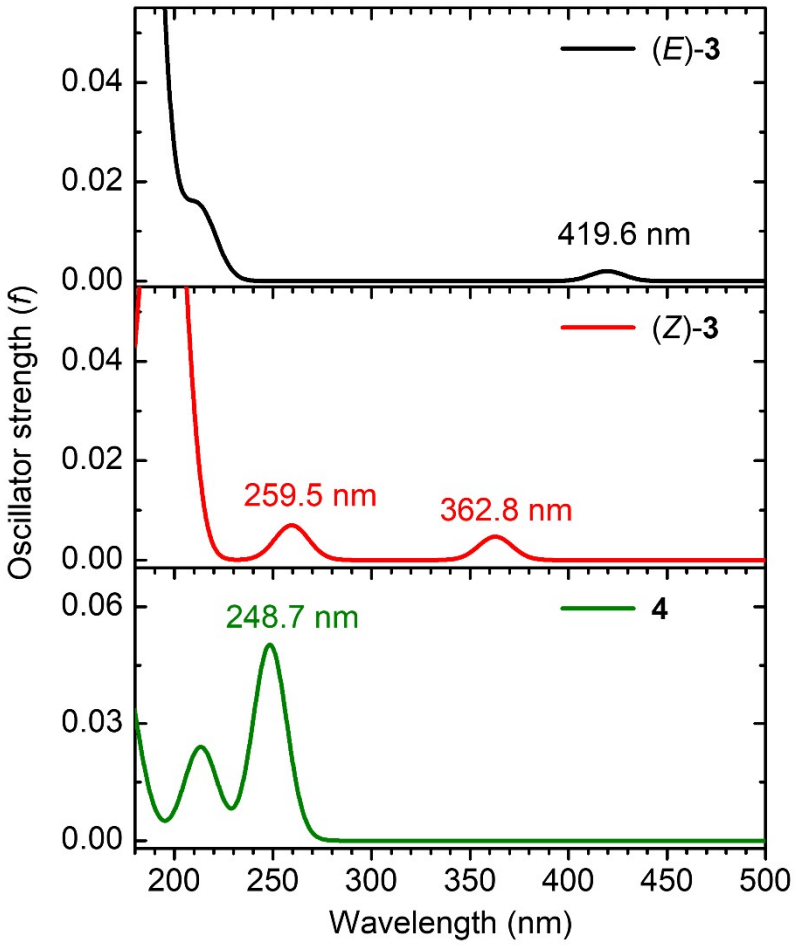


**Figure S3**. Simulated ultraviolet-visible spectra of (*E*)-**3**, (*Z*)-**3**, and **4** calculated at the TD-B3LYP/cc-pVTZ level of theory. The spectra were convoluted using a Gaussian function with a full width at half maximum of 20 nm.

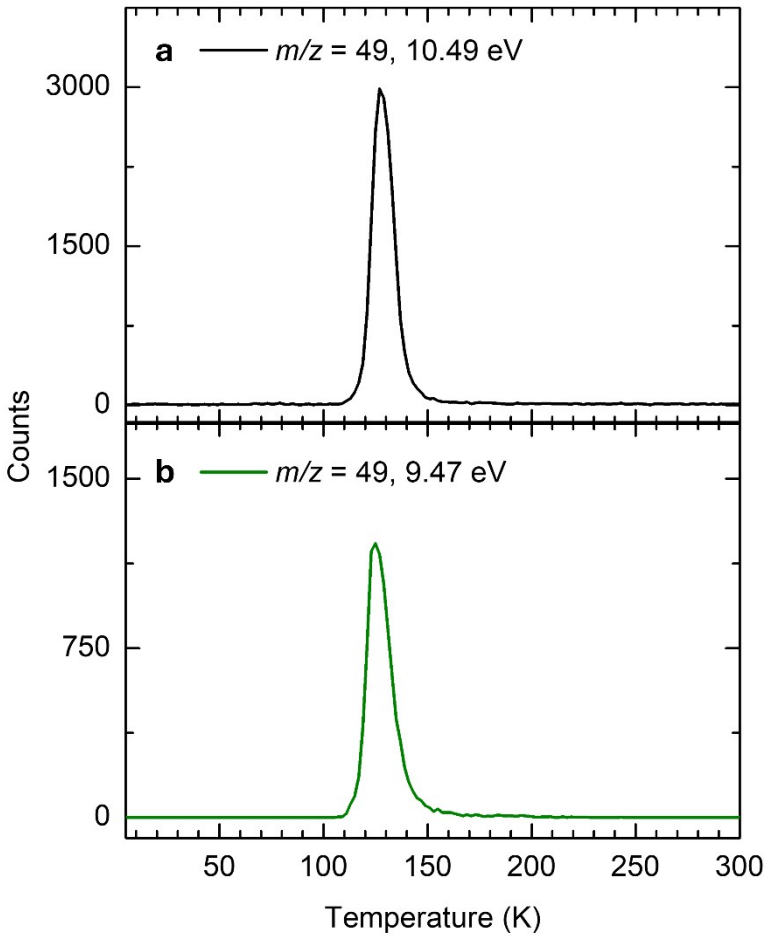


**Figure S4**. TPD profiles of ion signal at *m/z* = 49 from irradiated $PH_3$–$NH_3$ ices measured at 10.49 eV (a) and 9.47 eV (b).

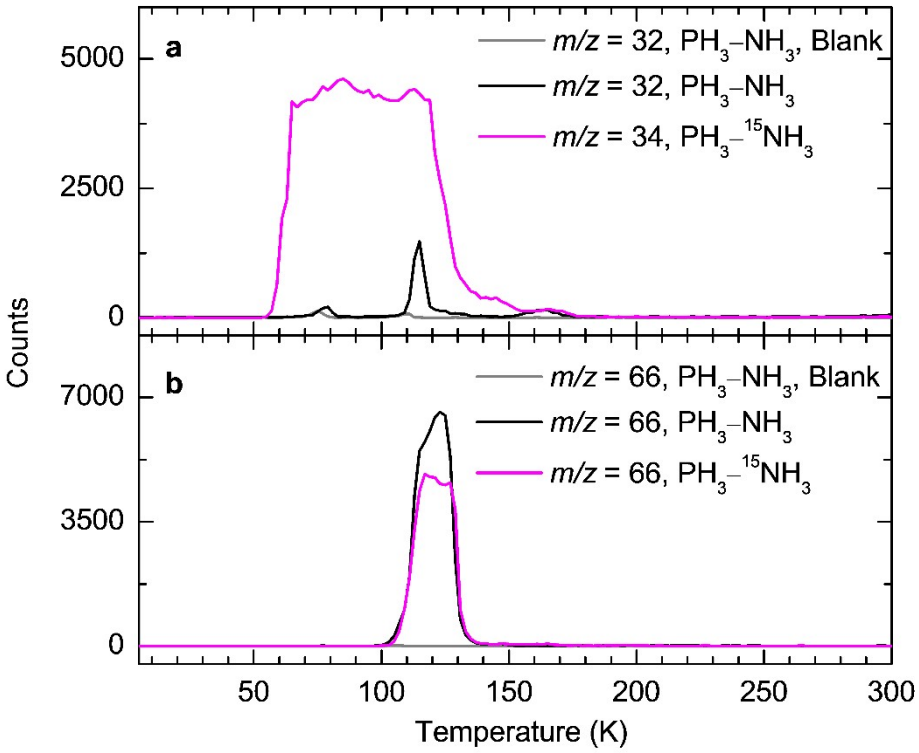


**Figure S5**. Ion signals of phosphine−ammonia ices recorded at 10.49 eV. TPD profiles of *m/z* = 32 and 34 from $PH_3$−$NH_3$ and $PH_3$−$^{15}NH_3$ ices, respectively (a), and *m/z* = 66 from both ices (b).

**Table S1**. Infrared absorption peaks of $PH_3$–$NH_3$ ice before and after electron irradiation at 5 K.

| Absorptions before irradiation ($cm^{-1}$) | |
|---|---|
| $PH_3$ | Assignment[3] |
| 2319 | $\nu_1$ or $\nu_3$ |
| 2199 | $2\nu_4$ |
| 1873 | $2\nu_2$ |
| 1091 | $\nu_4$ |
| 983 | $\nu_2$ |
| $NH_3$ | Assignment[23] |
| 4994 | $\nu_3 + \nu_4$ |
| 4470 | $\nu_2 + \nu_3$ |
| 3369 | $\nu_3$ |
| 3295 | $2\nu_4$ |
| 3207 | $\nu_1$ |
| 1632 | $\nu_4$ |
| 1051 | $\nu_2$ |
| New absorptions after irradiation ($cm^{-1}$) | Assignment |
| 2768 | $\nu_5(N{=}NH_2)$[24] |
| 2236 | P–H stretching[25] |
| 1504 | $\dot{N}H_2$ bending ($\nu_2$)[26,27] |
| 1100 | P=N stretching[2,25] |

**Table S2**. Error analysis of adiabatic ionization energies (IEs) and relative energies (ΔE) of $H_2PN$ isomers, computed at the MRCI/CBS//CCSD/cc-pVTZ level including CCSD/cc-pVTZ zero-point vibrational energy (ZPVE) corrections. IEs have been corrected for thermal and Stark effects by −0.03 eV, and an uncertainty of −0.03–+0.06 eV is applied.[20,21,28,29]

| Isomers | Structure | ΔE (kJ mol$^{-1}$) | Computed IE (eV) | Corrected IE ranges (eV) |
|---|---|---|---|---|
| (*E*)-**3** | 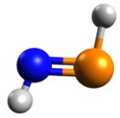 | 0 | 9.30 | 9.24–9.33 |
| (*Z*)-**3** | 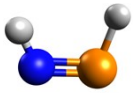 | 2 | 9.49 | 9.43–9.52 |
| **4** | 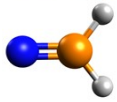 | 154 | 9.50 | 9.44–9.53 |
| **5** | 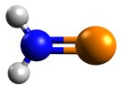 | 60 | 7.51[a] | 7.45–7.54 |

[a] Computed at both the CCSD(T)/CBS//CCSD/cc-pVTZ and CCSD(T)/CBS//B3LYP/cc-pVTZ levels of theory including CCSD/cc-pVTZ zero-point vibrational energy corrections.

**Table S3**. Generation parameters of vacuum ultraviolet (VUV) photons via four-wave mixing. The uncertainty in the VUV photon energy is less than 0.001 eV.

| VUV photon energy (eV) | Nonlinear medium | $\omega_1$ wavelength (nm) | $\omega_1$ dye | $\omega_2$ wavelength (nm) | $\omega_2$ dye |
|---|---|---|---|---|---|
| 10.49 ($3\omega_1$) | Xenon | 355 | – | – | – |
| 9.47 ($2\omega_1 - \omega_2$) | Krypton | 212.556 | Stilbene 420 | 564.583 | Rhodamine 590 |
| 9.39 ($2\omega_1 - \omega_2$) | Xenon | 222.566 | Coumarin450 | 707.956 | LDS 722 |
| 8.80 ($2\omega_1 - \omega_2$) | Xenon | 222.566 | Coumarin450 | 529.553 | Coumarin 540A |

**Table S4**. Optimized Cartesian coordinates (Å) on the adiabatic singlet ground state potential energy surfaces of $H_2PN$ isomers and their doublet cations calculated at the CCSD/cc-pVTZ level of theory. The point group symmetries and electronic ground states are provided.

| Atom | X | Y | Z | Atom | X | Y | Z |
|---|---|---|---|---|---|---|---|
| (*E*)-**3**, $C_s$, $^1$A' | | | | (*E*)-**3**$^+$, $C_s$, $^2$A' | | | |
| N | 0.018773 | 1.052725 | 0.000000 | N | 0.037199 | 0.996229 | 0.000000 |
| H | 0.982774 | 1.383485 | 0.000000 | H | 0.564618 | 1.863941 | 0.000000 |
| P | 0.018773 | -0.533713 | 0.000000 | P | 0.037199 | -0.538075 | 0.000000 |
| H | -1.395772 | -0.746863 | 0.000000 | H | -1.382987 | -0.766419 | 0.000000 |
| (*Z*)-**3**, $C_s$, $^1$A' | | | | (*Z*)-**3**$^+$, $C_1$, $^2$A | | | |
| N | 0.096378 | 1.049634 | 0.000000 | N | -1.000012 | 0.031246 | 0.000089 |
| H | -0.819576 | 1.487244 | 0.000000 | H | -1.989307 | 0.232937 | 0.000335 |
| P | 0.096378 | -0.528933 | 0.000000 | P | 0.509031 | -0.102073 | -0.000054 |
| H | -1.300747 | -0.900695 | 0.000000 | H | 1.353923 | 1.079444 | -0.000147 |
| **4**, $C_{2v}$, $^1$A$_1$ | | | | **4**$^+$, $C_{2v}$, $^2$B$_2$ | | | |
| N | 0.000000 | 0.000000 | -1.147109 | N | 0.000000 | 0.000000 | -1.179917 |
| P | 0.000000 | 0.000000 | 0.370466 | P | 0.000000 | 0.000000 | 0.401754 |
| H | 0.000000 | 1.115858 | 1.236384 | H | 0.000000 | 1.207376 | 1.116555 |
| H | 0.000000 | -1.115858 | 1.236384 | H | 0.000000 | -1.207376 | 1.116555 |
| **5**, $C_{2v}$, $^1$A$_1$ | | | | **5**$^+$, $C_{2v}$, $^2$B$_2$ | | | |
| N | 0.000000 | 0.000000 | -0.977843 | N | 0.000000 | 0.000000 | -0.952230 |
| P | 0.000000 | 0.000000 | 0.660692 | P | 0.000000 | 0.000000 | 0.645626 |
| H | 0.000000 | 0.842600 | -1.532740 | H | 0.000000 | 0.852667 | -1.509393 |
| H | 0.000000 | -0.842600 | -1.532740 | H | 0.000000 | -0.852667 | -1.509393 |

**Table S5**. Vibrational frequencies ($cm^{-1}$) and infrared intensities (km $mol^{-1}$) on the adiabatic singlet and doublet ground state potential energy surfaces of $H_2PN$ isomers and their cations, calculated at the CCSD/cc-pVTZ level of theory.

| Normal modes | Frequency | IR Intensity | Frequency | IR Intensity |
|---|---|---|---|---|
| | (*E*)-**3** | | (*E*)-**3**$^+$ | |
| 1 | 926.8322 | 33.811 | 530.1662 | 157.7359 |
| 2 | 998.2809 | 28.8542 | 688.7967 | 170.262 |
| 3 | 1064.5824 | 53.0309 | 788.2739 | 36.7129 |
| 4 | 1139.5247 | 29.0192 | 1163.0617 | 3.5618 |
| 5 | 2330.9726 | 136.0119 | 2240.5992 | 15.189 |
| 6 | 3504.0297 | 10.6255 | 3589.3726 | 356.8944 |
| | (*Z*)-**3** | | (*Z*)-**3**$^+$ | |
| 1 | 847.677 | 74.611 | 255.5807 | 167.4222 |
| 2 | 939.544 | 74.5941 | 445.193 | 102.1566 |
| 3 | 1070.9877 | 37.6657 | 521.522 | 134.0936 |
| 4 | 1115.8919 | 4.867 | 1172.1334 | 11.0599 |
| 5 | 2235.0898 | 203.6221 | 2080.9832 | 17.4441 |
| 6 | 3547.295 | 10.1056 | 3657.1472 | 437.3042 |
| | **4** | | **4**$^+$ | |
| 1 | 488.8626 | 6.7262 | 467.6598 | 22.5644 |
| 2 | 721.7778 | 4.7703 | 581.5668 | 21.1837 |
| 3 | 1193.7408 | 29.1273 | 995.023 | 7.6401 |
| 4 | 1276.4759 | 5.9864 | 1083.5237 | 6.0212 |
| 5 | 2415.913 | 26.2943 | 2478.0211 | 51.7574 |
| 6 | 2426.2114 | 96.6474 | 2544.7231 | 73.5081 |
| | **5** | | **5**$^+$ | |
| 1 | 726.2532 | 193.8062 | 818.4276 | 218.1815 |
| 2 | 972.8484 | 18.3953 | 863.7864 | 9.7536 |
| 3 | 985.3374 | 34.5608 | 1067.9055 | 20.0477 |
| 4 | 1642.6269 | 7.9384 | 1608.6829 | 65.7932 |
| 5 | 3538.6051 | 7.089 | 3464.7819 | 198.4898 |
| 6 | 3627.6642 | 40.4515 | 3559.685 | 173.9561 |

**Table S6**. Optimized Cartesian coordinates (Å) on the adiabatic singlet ground state potential energy surfaces of structures for reactions of $H_2PNH_2^+$ and $HNPH_3^+$ loss $H_2$ calculated at the CCSD/cc-pVTZ level of theory.

| Atom | X | Y | Z | Atom | X | Y | Z |
|---|---|---|---|---|---|---|---|
| **$H_2PNH_2^+$** | | | | **$HNPH_3^+$** | | | |
| H | 0.234825 | 1.575425 | -0.850829 | H | -0.898262 | 1.640139 | 0.000000 |
| H | 0.234825 | 1.575425 | 0.850829 | H | 0.744692 | -0.874673 | 1.131539 |
| H | -0.663915 | -0.977577 | 1.145140 | H | -1.202609 | -1.143801 | 0.000000 |
| H | -0.663915 | -0.977577 | -1.145140 | N | 0.027795 | 1.202636 | 0.000000 |
| N | 0.039008 | 1.063206 | 0.000000 | P | 0.027795 | -0.477696 | 0.000000 |
| P | 0.039008 | -0.575876 | 0.000000 | H | 0.744692 | -0.874673 | -1.131539 |
| **TS ($2^+$–$1^+$)** | | | | **TS ($1^+$ – $3^+$+$H_2$)** | | | |
| H | 0.466988 | -0.237807 | 1.169303 | H | 0.250301 | 1.203699 | 0.402138 |
| H | 1.630838 | 0.777726 | -0.014830 | H | 1.660162 | -0.728476 | 0.350081 |
| H | -1.132228 | -1.136270 | -0.455117 | H | -0.966741 | -0.505995 | 1.184034 |
| H | -1.223263 | 1.180337 | -0.291845 | H | -0.675913 | 1.405215 | 0.133811 |
| N | 1.137059 | -0.112502 | -0.138780 | N | 1.136208 | 0.052199 | -0.049306 |
| P | -0.513450 | 0.013568 | 0.037597 | P | -0.548084 | -0.115989 | -0.114995 |
| **TS ($1^+$ – $5^+$+$H_2$)** | | | | **TS ($2^+$ – $3^+$+$H_2$)** | | | |
| H | -1.650273 | -0.747031 | 0.180570 | H | 1.736040 | -0.655513 | 0.192363 |
| H | -1.541899 | 0.902964 | -0.210327 | H | -1.129310 | 1.166140 | -0.227060 |
| H | 0.889744 | 1.335132 | -0.338864 | H | -1.140765 | -0.920652 | 0.812993 |
| H | 0.899405 | 1.287358 | 0.558684 | N | 1.162007 | 0.175827 | 0.027060 |
| N | -1.048979 | 0.049572 | 0.010196 | P | -0.451306 | -0.124338 | -0.120746 |
| P | 0.583059 | -0.208362 | -0.017429 | H | -0.830420 | 1.044310 | 0.843483 |
| **TS ($2^+$– $4^+$+$H_2$)** | | | | | | | |
| H | 0.182743 | 1.324838 | -0.001247 | | | | |
| H | -1.100717 | -0.417536 | 1.167097 | | | | |
| H | -0.846581 | 1.459784 | -0.001185 | | | | |
| N | 1.236288 | -0.059963 | -0.000016 | | | | |
| P | -0.385816 | -0.101744 | 0.000038 | | | | |
| H | -1.102220 | -0.421188 | -1.165126 | | | | |

**Table S7**. Vibrational frequencies ($cm^{-1}$) and infrared intensities (km $mol^{-1}$) on the adiabatic singlet and doublet ground state potential energy surfaces of structures for reactions of $H_2PNH_2^+$ and $HNPH_3^+$ loss $H_2$ calculated at the CCSD/cc-pVTZ level of theory.

| | **$H_2PNH_2^+$** | | **$HNPH_3^+$** | |
|---|---|---|---|---|
| Normal modes | Frequency($cm^{-1}$) | IR Inten | Frequency($cm^{-1}$) | IR Inten |
| 1 | 410.43 | 9.0105 | 30.8 | 103.2913 |
| 2 | 575.85 | 206.5934 | 692.11 | 55.4508 |
| 3 | 755.29 | 1.5924 | 747.73 | 22.5744 |
| 4 | 755.45 | 38.8571 | 823.04 | 24.4976 |
| 5 | 969.54 | 10.9804 | 1035.25 | 30.9839 |
| 6 | 1041.32 | 31.4035 | 1066.4 | 35.3625 |
| 7 | 1061.08 | 14.7707 | 1107.65 | 14.607 |
| 8 | 1613.04 | 56.4178 | 1109.09 | 3.1584 |
| 9 | 2489.99 | 7.1706 | 2529.97 | 4.142 |
| 10 | 2542.74 | 6.5918 | 2568.09 | 12.4313 |
| 11 | 3545.22 | 241.9696 | 2569.52 | 20.4168 |
| 12 | 3651.22 | 164.3094 | 3476.75 | 99.4869 |
| | **TS ($2^+$–$1^+$)** | | **TS ($1^+$ – $3^+$+$H_2$)** | |
| 1 | -1992.92 | 255.6836 | -1701.29 | 104.6484 |
| 2 | 561.83 | 36.6491 | 498.28 | 127.9033 |
| 3 | 711.8 | 29.7022 | 582.76 | 2.2262 |
| 4 | 746.52 | 31.0977 | 719.65 | 46.8421 |
| 5 | 847.5 | 35.9993 | 838.77 | 21.4759 |
| 6 | 976.81 | 16.5059 | 958.69 | 30.5851 |
| 7 | 1042.22 | 30.4535 | 1012.08 | 15.4397 |
| 8 | 1080.09 | 17.9729 | 1249.2 | 25.0329 |
| 9 | 2075.39 | 92.2435 | 1877.39 | 57.0814 |
| 10 | 2492.04 | 9.7567 | 2090.46 | 4.7943 |
| 11 | 2574.85 | 20.9413 | 2405.64 | 0.1756 |
| 12 | 3465.94 | 118.2906 | 3500.7 | 125.1449 |
| | **TS ($1^+$ – $5^+$+$H_2$)** | | **TS ($2^+$ – $3^+$+$H_2$)** | |
| 1 | -464.92 | 31.4303 | -1299.15 | 298.3147 |
| 2 | 477.71 | 206.4676 | 452.04 | 89.4079 |
| 3 | 596.49 | 0.8764 | 636.6 | 43.5299 |
| 4 | 673.09 | 30.862 | 651.63 | 21.1891 |

| | | | | |
|---|---|---|---|---|
| 5 | 853.65 | 3.6477 | 831.92 | 13.1039 |
| 6 | 925.59 | 17.6001 | 872.32 | 49.7817 |
| 7 | 944.28 | 28.5095 | 1016.95 | 29.2595 |
| 8 | 1586.15 | 11.6534 | 1113.14 | 17.0656 |
| 9 | 1612.09 | 58.3859 | 1831 | 13.8934 |
| 10 | 2455.79 | 24.5941 | 2281.42 | 77.9977 |
| 11 | 3551.42 | 243.0053 | 2482.19 | 23.668 |
| 12 | 3660.51 | 151.6562 | 3487.34 | 127.236 |
| | **TS ($2^{+}$– $4^{+}$+$H_2$)** | | | |
| 1 | -2112.77 | 813.1127 | | |
| 2 | 401.2 | 0.2232 | | |
| 3 | 700.19 | 8.3132 | | |
| 4 | 872.37 | 22.6323 | | |
| 5 | 931.73 | 2.0936 | | |
| 6 | 981.05 | 10.913 | | |
| 7 | 1015.24 | 11.0967 | | |
| 8 | 1181.02 | 41.8472 | | |
| 9 | 1815.97 | 286.5772 | | |
| 10 | 2068.27 | 81.0045 | | |
| 11 | 2479.09 | 11.9515 | | |
| 12 | 2521.8 | 24.1013 | | |

**Table S8**. Optimized Cartesian coordinates (Å) on the adiabatic singlet ground state potential energy surfaces of $H_4PN$ structures in Fig. 6 calculated at the CCSD/cc-pVTZ level of theory.

| Atom | X | Y | Z | Atom | X | Y | Z |
|---|---|---|---|---|---|---|---|
| **1**, $C_1$, $^1A$ | | | | **2**, $C_s$, $^1A'$ | | | |
| H | -1.590567 | -0.805598 | 0.157990 | H | -0.526942 | -1.172624 | 1.069693 |
| H | -1.521870 | 0.824804 | 0.400477 | H | -0.891678 | 1.563156 | 0.000000 |
| H | 0.949698 | 0.448048 | 1.227779 | H | 1.346327 | -0.884140 | 0.000000 |
| H | 0.946991 | 1.049112 | -0.743897 | H | -0.526942 | -1.172624 | -1.069693 |
| N | -1.110699 | 0.044797 | -0.085541 | N | 0.027238 | 1.142376 | 0.000000 |
| P | 0.599376 | -0.121996 | -0.029571 | P | 0.027238 | -0.422026 | 0.000000 |
| **6**, $C_s$, $^1A'$ | | | | **$H_2PNH$**, $C_1$, $^2A$ | | | |
| H | 0.393258 | 1.538511 | 0.823901 | H | -1.585953 | 0.764574 | -0.028439 |
| H | 1.370162 | -0.760186 | 0.000000 | H | 0.997381 | -1.086226 | 0.605471 |
| H | -1.017150 | 1.460502 | 0.000000 | H | 0.968984 | 1.059053 | 0.728161 |
| H | 0.393258 | 1.538511 | -0.823901 | N | -1.132849 | -0.143271 | 0.060914 |
| P | -0.051797 | -0.790228 | 0.000000 | P | 0.503302 | 0.017700 | -0.115440 |
| N | -0.051797 | 1.153725 | 0.000000 | H | -1.585953 | 0.764574 | -0.028439 |
| **$HPNH_2$**, $C_1$, $^2A$ | | | | **TS (1 – 3+$H_2$)** | | | |
| H | -0.866304 | 1.301956 | -0.046330 | H | 0.197167 | 1.256935 | -0.101280 |
| H | 1.577117 | -0.812570 | 0.143328 | H | 1.577112 | -0.273591 | -0.674707 |
| H | 1.525181 | 0.854119 | 0.237641 | H | -1.026044 | 0.049811 | 1.211454 |
| P | -0.642441 | -0.099122 | 0.010780 | H | -0.741003 | 1.531752 | -0.244643 |
| N | 1.057232 | 0.020474 | -0.070905 | N | 1.103424 | 0.004219 | 0.180679 |
| | | | | P | -0.515413 | -0.172963 | -0.097038 |
| **TS (2 – 3+$H_2$)** | | | | **TS (6 – 3+$H_2$)** | | | |
| H | 1.640051 | 0.507556 | 0.503469 | H | -0.886623 | 1.242753 | -0.483733 |
| H | -1.090084 | -1.125891 | -0.416267 | H | 1.402504 | -0.975158 | 0.041420 |
| H | -1.407605 | 0.992526 | 0.051807 | H | 1.584649 | 0.654584 | -0.264419 |
| N | 1.145255 | -0.020780 | -0.206834 | P | -0.725890 | -0.048819 | 0.085146 |
| P | -0.390122 | -0.057792 | 0.157192 | N | 0.913857 | -0.131028 | -0.215015 |
| H | -1.307312 | 0.638142 | -1.049060 | H | 2.390821 | 0.727307 | 0.934649 |

**Table S9.** Vibrational frequencies ($cm^{-1}$) and infrared intensities (km $mol^{-1}$) on the adiabatic singlet ground state potential energy surfaces of $H_4PN$ structures.

| | **1** | | **2** | |
|---|---|---|---|---|
| Normal modes | Frequency($cm^{-1}$) | IR Inten | Frequency($cm^{-1}$) | IR Inten |
| 1 | 352.0043 | 20.6906 | 391.0997 | 103.327 |
| 2 | 555.6901 | 182.0434 | 784.5421 | 93.9638 |
| 3 | 833.9631 | 28.5677 | 791.5615 | 12.4935 |
| 4 | 862.4771 | 6.0879 | 923.661 | 78.6539 |
| 5 | 938.5796 | 33.6942 | 1119.1774 | 21.6473 |
| 6 | 1103.9535 | 34.2501 | 1135.564 | 8.9938 |
| 7 | 1179.6733 | 27.7275 | 1165.3115 | 37.0327 |
| 8 | 1635.2708 | 19.16 | 1238.9183 | 152.5785 |
| 9 | 2362.3737 | 130.2845 | 2367.1094 | 147.7712 |
| 10 | 2426.8186 | 84.5375 | 2400.5544 | 149.037 |
| 11 | 3591.8528 | 9.2124 | 2546.2275 | 35.1502 |
| 12 | 3689.459 | 22.7512 | 3615.5018 | 16.4082 |
| | **6** | | | |
| 1 | 192.455 | 2.638 | | |
| 2 | 511.1066 | 18.9833 | | |
| 3 | 675.4189 | 3.1938 | | |
| 4 | 744.2512 | 15.2505 | | |
| 5 | 1004.996 | 42.0391 | | |
| 6 | 1321.8389 | 76.7591 | | |
| 7 | 1678.1218 | 28.1582 | | |
| 8 | 1687.2321 | 30.7176 | | |
| 9 | 2376.166 | 137.2136 | | |
| 10 | 3498.4107 | 13.4492 | | |
| 11 | 3603.9601 | 71.8222 | | |
| 12 | 3614.1265 | 52.3658 | | |
| | **$H_2PNH$** | | **$HPNH_2$** | |
| 1 | 374.1405 | 108.8495 | 374.1405 | 108.8495 |
| 2 | 449.1162 | 110.1364 | 449.1162 | 110.1364 |
| 3 | 817.7606 | 6.1604 | 817.7606 | 6.1604 |
| 4 | 868.7151 | 49.4187 | 868.7151 | 49.4187 |
| 5 | 1092.3873 | 32.6204 | 1092.3873 | 32.6204 |
| 6 | 1617.2749 | 26.1365 | 1617.2749 | 26.1365 |
| 7 | 2398.5841 | 94.8079 | 2398.5841 | 94.8079 |
| 8 | 3611.9792 | 28.0282 | 3611.9792 | 28.0282 |

| | | | | |
|---|---|---|---|---|
| 9 | 3721.5063 | 32.9869 | 3721.5063 | 32.9869 |
| | **TS (1 – 3+$H_2$)** | | **TS (2 – 3+$H_2$)** | |
| 1 | -2270.9958 | 540.662 | -1532.8036 | 227.326 |
| 2 | 605.8949 | 26.8432 | 370.3654 | 47.2684 |
| 3 | 746.838 | 166.8139 | 689.7256 | 7.6128 |
| 4 | 916.694 | 24.4485 | 764.712 | 18.4564 |
| 5 | 948.7276 | 109.5384 | 916.1223 | 78.2181 |
| 6 | 1034.8644 | 12.6836 | 988.3745 | 84.5608 |
| 7 | 1145.4046 | 26.2071 | 1128.4774 | 10.9043 |
| 8 | 1152.3932 | 36.9452 | 1233.5152 | 50.0244 |
| 9 | 1746.1302 | 574.3579 | 1467.6316 | 384.8665 |
| 10 | 2030.6465 | 25.6896 | 2236.7761 | 12.9739 |
| 11 | 2377.2635 | 98.7605 | 2527.1451 | 14.0383 |
| 12 | 3523.1808 | 9.2119 | 3570.084 | 20.3612 |
| | **TS (6 – 3+$H_2$)** | | | |
| 1 | -755.6768 | 393.229 | | |
| 2 | 443.6232 | 18.3514 | | |
| 3 | 474.3493 | 32.5702 | | |
| 4 | 655.5297 | 88.1966 | | |
| 5 | 761.7058 | 22.5909 | | |
| 6 | 829.886 | 11.1684 | | |
| 7 | 917.1228 | 14.1732 | | |
| 8 | 1083.0024 | 42.6138 | | |
| 9 | 1555.9797 | 63.6455 | | |
| 10 | 2399.1647 | 86.4143 | | |
| 11 | 3150.247 | 392.1973 | | |
| 12 | 3645.585 | 47.303 | | |

**Table S10.** $T_1$ diagnostic values for species in Figs. 1, 4, and 6.

| | | $T_1$ diagnostic | | |
|---|---|---|---|---|
| | | **CCSD(T)/ cc-pVDZ** | **CCSD(T)/ cc-pVTZ** | **CCSD(T)/ cc-pVQZ** |
| | **close-shell** | | | |
| 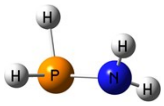 | **1 ($C_1$, $^1A$)** | 0.009966 | 0.010834 | 0.011321 |
| 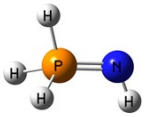 | **2 ($C_s$, $^1A'$)** | 0.015498 | 0.014376 | 0.014000 |
| 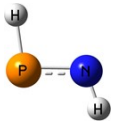 | (*E*)-**3 ($C_s$, $^1A'$)** | 0.015686 | 0.016129 | 0.016064 |
| 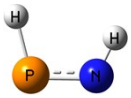 | (*Z*)-**3 ($C_s$, $^1A'$)** | 0.015572 | 0.016028 | 0.016037 |
| 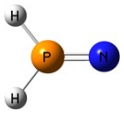 | **4 ($C_{2v}$, $^1A_1$)** | 0.029353 | 0.027809 | 0.027498 |
| 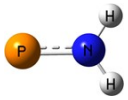 | **5 ($C_{2v}$, $^1A_1$)** | 0.019273 | 0.018007 | 0.017523 |
| 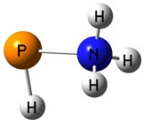 | **6 ($C_s$, $^1A'$)** | 0.009595 | 0.010554 | 0.011004 |
| 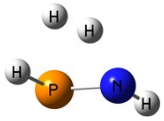 | **ts (1–3+$H_2$) ($C_1$, $^1A$)** | 0.017680 | 0.016237 | 0.015919 |
| 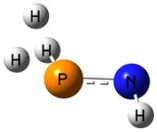 | **ts (2–3+$H_2$) ($C_1$, $^1A$)** | 0.020013 | 0.018104 | 0.017438 |

| | | | | |
|---|---|---|---|---|
| 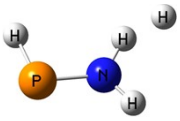 | **ts (6–3+$H_2$) ($C_1$, $^1$A)** | 0.054369 | 0.061301 | 0.063474 |
| | **open-shell** | | | |
| 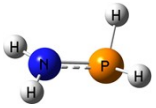 | **$1^+$ ($C_s$, $^2$A')** | 0.016338 | 0.017531 | 0.017641 |
| 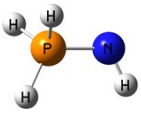 | **$2^+$ ($C_s$, $^2$A'')** | 0.014171 | 0.014703 | 0.014980 |
| 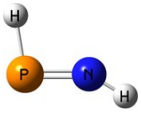 | (*E*)-**$3^+$ ($C_s$, $^2$A')** | 0.057876 | 0.0569701 | 0.057386 |
| 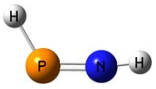 | (*Z*)-**$3^+$ ($C_1$, $^2$A)** | 0.063102 | 0.062664 | 0.063196 |
| 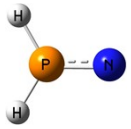 | **$4^+$ ($C_{2v}$, $^2B_2$)** | 0.072590 | 0.072067 | 0.072529 |
| 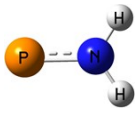 | **$5^+$ ($C_{2v}$, $^2B_2$)** | 0.024127 | 0.023162 | 0.023150 |
| 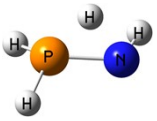 | **ts ($2^+$–$1^+$) ($C_1$, $^2$A)** | 0.025363 | 0.025945 | 0.026086 |
| 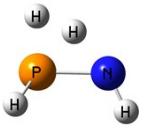 | **ts ($1^+$–$3^+$+$H_2$) ($C_1$, $^2$A)** | 0.027859 | 0.029022 | 0.029692 |
| 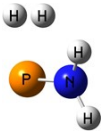 | **ts ($1^+$–$5^+$+$H_2$) ($C_1$, $^2$A)** | 0.017873 | 0.018728 | 0.018866 |

| | | | | |
|---|---|---|---|---|
| 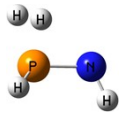 | **ts ($2^+$–$3^+$+$H_2$) ($C_1$, $^2$A)** | 0.023505 | 0.025089 | 0.025806 |
| 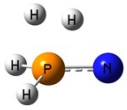 | **ts ($2^+$–$4^+$+$H_2$) ($C_1$, $^2$A)** | 0.028315 | 0.027243 | 0.027216 |
| 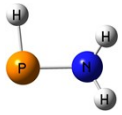 | **$HPNH_2$ ($C_1$, $^2$A)** | 0.016420 | 0.017537 | 0.017954 |
| 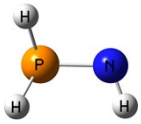 | **$H_2PNH$ ($C_1$, $^2$A)** | 0.028877 | 0.031339 | 0.032808 |

**Table S11. (a)** MRCI/CBS//CCSD/cc-pVTZ ionization energies (IE) of $H_2NP$ isomers depicted in Figure 1, and the activation energy of **6**→**3**+$H_2$ in Figure 6. **(b)** Numbers of configuration state functions (CSFs) of MCSCF and MRCI in **(a)**.

**(a)**

| | $E_{zpc}$[a] | MCSCF (6,9)/(5,9) | | | MRCI | | | | IE[b] (eV) | $E_a$[c] (kJ mol$^{-1}$) |
|---|---|---|---|---|---|---|---|---|---|---|
| | | cc-pVDZ | cc-pVTZ | cc-pVQZ | cc-pVDZ | cc-pVTZ | cc-pVQZ | CBS | | |
| (*E*)-**3** ($C_s$, $^1$A') | 0.022700 | -396.400972 | -396.441700 | -396.452456 | -396.639616 | -396.793463 | -396.851470 | -396.885362 | 9.30 | 0 |
| (*E*)-**3**$^+$ ($C_s$, $^2$A') | 0.020504 | -396.072866 | -396.112247 | -396.122140 | -396.311832 | -396.455057 | -396.509489 | -396.541332 | | |
| (*Z*)-**3** ($C_s$, $^1$A') | 0.022227 | -396.399009 | -396.439570 | -396.450182 | -396.638070 | -396.792229 | -396.850171 | -396.884008 | 9.49 | 2 |
| (*Z*)-**3**$^+$ ($C_1$, $^2$A) | 0.018527 | -396.065053 | -396.105594 | -396.115799 | -396.300348 | -396.444932 | -396.499688 | -396.531702 | | |
| **4** ($C_{2v}$, $^1A_1$) | 0.019417 | -396.355051 | -396.399510 | -396.412161 | -396.572309 | -396.728651 | -396.788359 | -396.823315 | 9.50 | 154 |
| **4**$^+$ ($C_{2v}$, $^2B_2$) | 0.018568 | -396.038569 | -396.077345 | -396.088117 | -396.248794 | -396.387900 | -396.441660 | -396.473193 | | |
| | | | | | | | | | | $E_a$[d] (kJ mol$^{-1}$) |
| **6** ($C_s$, $^1$A') | 0.047632 | -397.529162 | -397.570880 | -397.580950 | -397.808232 | -397.973379 | -398.032089 | -398.066064 | | 0 |
| **ts (6**–**3**+$H_2$) ($C_1$, $^1$A) | 0.036260 | -397.444859 | -397.488248 | -397.499067 | -397.734213 | -397.896305 | -397.953317 | -397.986248 | | 180 |

[a] zero-point energy by CCSD/cc-pVTZ in hartree,

[b] ionization energy by MRCI/CBS with CCSD/cc-pVTZ zero-point energy correction in eV,

[c] the relative energy of different isomer sets by MRCI/CBS with CCSD/cc-pVTZ zero-point energy correction in kJ mol$^{-1}$,

[d] activation energy by MRCI/CBS with CCSD/cc-pVTZ zero-point energy correction in kJ mol$^{-1}$.

**(b)**

| | MCSCF (6,9)/(5,9) | | | MRCI | | |
|---|---|---|---|---|---|---|
| | **cc-pVDZ** | **cc-pVTZ** | **cc-pVQZ** | **cc-pVDZ** | **cc-pVTZ** | **cc-pVQZ** |
| (*E*)-**3** ($C_s$, $^1$A') | 1,316 | 1,316 | 1,316 | 63,277,540 | 545,860,596 | 2,345,519,228 |
| (*E*)-**3**$^+$ ($C_s$, $^2$A') | 980 | 980 | 980 | 53,177,458 | 449,749,330 | 1,921,768,482 |
| (*Z*)-**3** ($C_s$, $^1$A') | 1,316 | 1,316 | 1,316 | 63,277,540 | 545,860,596 | 2,345,519,228 |
| (*Z*)-**3**$^+$ ($C_1$, $^2$A) | 1,890 | 1,890 | 1,890 | 176,854,500 | 1,582,487,100 | 6,926,064,660 |
| **4** ($C_{2v}$, $^1A_1$) | 684 | 684 | 684 | 18,426,930 | 150,905,992 | 638,250,340 |
| **4**$^+$ ($C_{2v}$, $^2B_2$) | 488 | 488 | 488 | 15,370,906 | 123,007,690 | 516,818,562 |
| **5** ($C_{2v}$, $^1A_1$) | 684 | 684 | 684 | 18,426,930 | 150,905,992 | 639,701,918 |
| **6** ($C_s$, $^1$A') | 1,316 | 1,316 | 1,316 | 137,250,912 | 1,195,242,982 | 5,297,582,236 |
| **ts (6–3**+$H_2$) ($C_1$, $^1$A) | 2,520 | 2,520 | 2,520 | 482,909,400 | 4,366,584,900 | 19,608,107,310 |

## References


1 B. M. Jones and R. I. Kaiser, *J. Phys. Chem. Lett.*, 2013, **4**, 1965-1971.
2 C. Zhu, A. Bergantini, S. K. Singh, R. I. Kaiser, A. K. Eckhardt, P. R. Schreiner, Y.-S. Huang, B.-J. Sun and A. H. H. Chang, *ChemComm.*, 2021, **57**, 4958-4961.
3 A. M. Turner, M. J. Abplanalp, S. Y. Chen, Y. T. Chen, A. H. H. Chang and R. I. Kaiser, *Phys. Chem. Chem. Phys.*, 2015, **17**, 27281-27291.
4 M. Bouilloud, N. Fray, Y. Benilan, H. Cottin, M. C. Gazeau and A. Jolly, *Mon. Not. R. Astron. Soc.*, 2015, **451**, 2145-2160.
5 S. A. Sandford and L. J. Allamandola, *Astrophys. J.*, 1993, **417**, 815.
6 R. I. Kaiser and K. Roessler, *Astrophys. J.*, 1997, **475**, 144.
7 D. Drouin, A. R. Couture, D. Joly, X. Tastet, V. Aimez and R. Gauvin, *Scanning*, 2007, **29**, 92-101.
8 A. G. Yeghikyan, *Astrophysics*, 2011, **54**, 87-99.
9 M. D. Francia and E. R. Nixon, *J. Chem. Phys.*, 1973, **58**, 1061-1065.
10 J. Wang, J. H. Marks, A. M. Turner, A. A. Nikolayev, V. Azyazov, A. M. Mebel and R. I. Kaiser, *Phys. Chem. Chem. Phys.*, 2023, **25**, 936-953.
11 G. D. Purvis III and R. J. Bartlett, *J. Chem. Phys.*, 1982, **76**, 1910-1918.
12 C. Hampel, K. A. Peterson and H.-J. Werner, *Chem. Phys. Lett.*, 1992, **190**, 1-12.
13 P. J. Knowles, C. Hampel and H. J. Werner, *J. Chem. Phys.*, 1993, **99**, 5219-5227.
14 M. J. Deegan and P. J. Knowles, *Chem. Phys. Lett.*, 1994, **227**, 321-326.
15 K. A. Peterson, D. E. Woon and T. H. D. Jr., *J. Chem. Phys.*, 1994, **100**, 7410-7415.
16 T. J. Lee and P. R. Taylor, *Int. J. Quantum Chem.*, 1989, **36**, 199-207.
17 J. C. Rienstra-Kiracofe, W. D. Allen and H. F. Schaefer, *J. Phys. Chem. A*, 2000, **104**, 9823-9840.
18 G. W. T. M. J. Frisch, H. B. Schlegel, G. E. Scuseria, M. A. Robb, J. R. Cheeseman, G. Scalmani, V. Barone, G. A. Petersson, H. Nakatsuji, X. Li, M. Caricato, A. V. Marenich, J. Bloino, B. G. Janesko, R. Gomperts, B. Mennucci, H. P. Hratchian, J. V. Ortiz, A. F. Izmaylov, J. L. Sonnenberg, D. Williams-Young, F. Ding, F. Lipparini, F. Egidi, J. Goings, B. Peng, A. Petrone, T. Henderson, D. Ranasinghe, V. G. Zakrzewski, J. Gao, N. Rega, G. Zheng, W. Liang, M. Hada, M. Ehara, K. Toyota, R. Fukuda, J. Hasegawa, M. Ishida, T. Nakajima, Y. Honda, O. Kitao, H. Nakai, T. Vreven, K. Throssell, J. A. Montgomery, Jr., J. E. Peralta, F. Ogliaro, M. J. Bearpark, J. J. Heyd, E. N. Brothers, K. N. Kudin, V. N. Staroverov, T. A. Keith, R. Kobayashi, J. Normand, K. Raghavachari, A. P. Rendell, J. C. Burant, S. S. Iyengar, J. Tomasi, M. Cossi, J. M. Millam, M. Klene, C. Adamo, R. Cammi, J. W. Ochterski, R. L. Martin, K. Morokuma, O. Farkas, J. B. Foresman, D. J. Fox, Gaussian 16, Revision C.1, Gaussian Inc. Wallingford, CT, 2019.
19 P. J. K. H.-J. Werner, G. Knizia, F. R. Manby, M. Schütz, P. Celani, W. Györffy, D. Kats, T. Korona, R. Lindh, A. Mitrushenkov, G. Rauhut, K. R. Shamasundar, T. B. Adler, R. D. Amos, S. J. Bennie, A. Bernhardsson, A. Berning, D. L. Cooper, M. J. O. Deegan, A. J. Dobbyn, F. Eckert, E. Goll, C. Hampel, A. Hesselmann, G. Hetzer, T. Hrenar, G. Jansen, C. Köppl, S. J. R. Lee, Y. Liu, A. W. Lloyd, Q. Ma, R. A. Mata, A. J. May, S. J. McNicholas, W. Meyer, T. F. Miller III, M. E. Mura, A. Nicklass, D. P. O'Neill, P. Palmieri, D. Peng, T. Petrenko, K. Pflüger, R. Pitzer, M. Reiher, T. Shiozaki, H. Stoll, A. J. Stone, R. Tarroni, T. Thorsteinsson, M. Wang, M. Welborn, and B. Ziegler, MOLPRO, 2024.1, a package of ab initio programs, University of Cardiff: Cardiff, U.K., 2024.
20 J. Wang, C. Zhang, A. K. Eckhardt and R. I. Kaiser, *Chem. Sci.*, 2025, **16**, 21111-21120.

21 Y. Mo, J. Yang and G. Chen, *J Chem Phys*, 2004, **120**, 1263-1270.
22 W. Zheng and R. I. Kaiser, *J. Phys. Chem. A*, 2010, **114**, 5251-5255.
23 W. Zheng and R. I. Kaiser, *Chem. Phys. Lett.*, 2007, **440**, 229-234.
24 J. H. Teles, G. Maier, B. Andes Hess Jr. and L. J. Schaad, *Chem. Ber.*, 1989, **122**, 749-752.
25 G. Socrates, *Infrared and raman characteristic group frequencies: Tables and charts*, 3rd edn., John Wiley & Sons, Ltd., New York, 2004.
26 D. E. Milligan and M. E. Jacox, *J. Chem. Phys.*, 1965, **43**, 4487-4493.
27 W. Zheng, D. Jewitt, Y. Osamura and R. I. Kaiser, *Astrophys. J.*, 2008, **674**, 1242.
28 R. Frigge, C. Zhu, A. M. Turner, M. J. Abplanalp, B.-J. Sun, Y.-S. Huang, A. H. Chang and R. I. Kaiser, *ChemComm.*, 2018, **54**, 10152-10155.
29 R. I. Kaiser, S. P. Krishtal, A. M. Mebel, O. Kostko and M. Ahmed, *Astrophys. J.*, 2012, **761**, 178.